

MODELING DEVELOPMENTS ON COLLOID THRUSTERS.

Jorge A. Carretero^a Francisco J. Higuera^b Manuel Martinez-Sanchez^c

^a*Department of Aeronautics and Astronautics
Massachusetts Institute of Technology, Cambridge, MA 02139
Email: jorgcb@mit.edu*

^b*E.T.S Ingenieros Aeronauticos, Madrid Spain,
Email: h@tupi.dmt.upm.es*

^c*Department of Aeronautics and Astronautics
Massachusetts Institute of Technology, Cambridge, MA 02139
Email: mmart@mit.edu*

Abstract

The renewed interest in colloidal thruster technology for micropropulsion applications has rekindled research on the physics of these electrically driven jets. In this paper we address two aspects of this topic. Firstly, from a numerical perspective, we explore the cone-jet transition region for a Formamide solution near the minimum flow limit ($\eta \approx 1$). Secondly, from an analytical standpoint, we study the movement of charges within the colloidal jet and its effect on the non-neutral layer thickness.

Numerical results have been obtained for a Formamide solution with conductivity $K = 10^{-3} Si/m$ for low flow rates $1 \leq \eta \leq 4$. Our simulation is shown to conserve mass, charge and energy and our results show good agreement with published experimental data. For a high dielectric constant, the results also show finite conduction currents in the jet and a weak dependence of the convection current on flow rate.

Analytical estimates have been obtained for the non-neutral and ambipolar layers created by an electrical field normal to the liquid surface. It is shown that the non-neutral layer is thin compared to the liquid jet. This result justifies the use of a constant conductivity in numerical models.

1 Introduction

The basic physics of colloidal thrusters have been addressed in numerous experimental and theoretical papers. These papers have successfully yielded basic scaling laws for the cone and jet regions as seen in the works of Fernandez de la Mora [1], Hohman[2], and Martinez-Sanchez [3] to name a few. However, the transition region from the cone to the free jet, see Figure 1, has proven exceptionally difficult to model accurately. Some of the difficulties reside on various factors including the strong coupling between the fluid mechanics and electrostatic aspects of the problem, the strong gradients observed, and the uncertainty over the behavior of the electrical charges in the fluid. A better understanding of this transition is critical in order to explain the physics of the electrospray current, predict droplet size, and explore the minimum flow rate stability threshold.

In recent years several numerically based models have been presented to simulate the cone-jet transition region. The numerical work in this area may be traced back to the model of Eggers

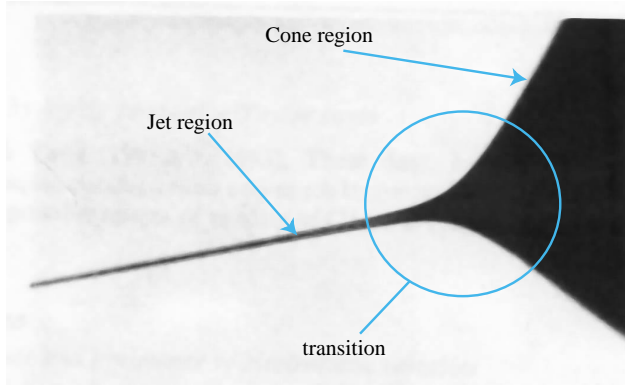


Fig. 1. Structure of the cone jet for Ethylene-Glycol, $\eta = 2, \text{Re}=10.2$, courtesy of Fernandez de la Mora [1]

and Dupont for gravity and pressure driven fluid jets[5]. The success of this and subsequent models suggested that a similar approach could be used for electrified jets. As of this writing several models have been published such as the works of Hohmann *et al*[2], Hartmann *et al* [4] and Yan *et al*,[10]. The model presented by Hartmann computes the cone and jet shape, the electric fields inside and outside of the cone, and the surface charge density. Hartmann's model uses a one dimensional flow approximation. Yan's model is similar to that of Hartmann, but assumes an axisymmetric parabolic velocity profile. The model presented by Hohmann and coworkers is also based on cylindrical coordinates but assumes that the jet is long and slender, thus allowing for a perturbative expansion in the aspect ratio.

In this paper we present the results from our quasi-one-dimensional cone-jet model. In particular we show results for higher electrical conductivities than those published before ($K = 10^{-3} \text{Si/m}$), we also show results for low flow rates ($\eta \approx 1.3$), and we explore the effect of parameter changes on flow variables. We also present a detailed study of the thickness of the non-neutral layer in the jet, which justifies the use of a constant conductivity in numerical models of the cone-jet regime.

2 Cone-jet numerical model

In our case the cone-jet model formulation is based on local spherical symmetry. The model assumes that the jet is axisymmetric, slender, quasi-one dimensional, and unsteady. A explicit multistage fourth order Runge-Kutta scheme (*RK4*) is employed to time march the simulation. The *RK4* scheme, like other explicit schemes, is easy to implement and yields information on the dynamics of the cone-jet structure.

The system of equations solved includes : mass conservation, momentum conservation, internal charge conservation, surface charge relaxation, an electrostatic boundary surface element solver, as described by [8], and the system is closed by specifying two local surface boundary conditions. The equations and their detailed explanation can be found in [6].

In this paper we only reproduce the surface boundary conditions due to changes we have made in their formulation. For the normal direction boundary condition the normal electrical stress term is given by [7]

$$\tau_{nm} = \frac{\epsilon_0}{2} [(E_n^o)^2 - \epsilon(E_n^i)^2 + \epsilon - 1)E_t^2] \quad (1)$$

where ϵ_0 is the permittivity of free space, ϵ is the relative permittivity, E_n^o the normal external electric field intensity, E_n^i the internal normal electrical field, and E_t the tangential electrical field. The normal stress balance boundary condition is now given by

$$P_0 = \gamma \left(\frac{1}{h \left(1 + \left(\frac{\partial h}{\partial z}\right)^2\right)^{0.5}} - \frac{\frac{\partial^2 h}{\partial z^2}}{\left(1 + \left(\frac{\partial h}{\partial z}\right)^2\right)^{1.5}} \right) + \mu \left(\frac{2\alpha u'}{h} - \frac{\partial u}{\partial z} \right) - \frac{\epsilon_0}{2} [(E_n^o)^2 - \epsilon(E_n^i)^2 + (\epsilon - 1)E_t^2] \quad (2)$$

where γ is the surface tension coefficient, μ is the fluid viscosity, P_0 , is the pressure at the axis, and h is the local jet radius, u' is the shear velocity defined as $u' = (u_\alpha - u_0)/2$, $u = (u_\alpha + u_0)/2$ is the mean velocity, u_α is the flow velocity at the jet surface and u_0 is the flow velocity at the jet axis. The tangential boundary condition is obtained in the same fashion and contains contributions from the viscous shear stresses and the corresponding tangential electrical stress.

$$u' = \frac{\sigma E_t h}{4\mu}. \quad (3)$$

The electrostatic boundary surface element solver has been modified from its original form (as presented by Lozano *et al*[8]). In Lozano's case the electrical charges were assumed to be fully relaxed, so that $\sigma = \epsilon_0 E_n^o$. In our case the liquid is not fully relaxed and the liquid potential is now calculated by

$$\phi = B(V) + A(E_n^o - E_n^{in}) \quad (4)$$

where the vector B comprises the effect of charges on the needle on the liquid potential and the full matrix A the effect of liquid charges on the liquid potential[8]. In the case of Lozano and coworkers the normal internal electric field (E_n^{in}) was identically zero, whereas in our case it is calculated by $E_n^{in} = ((E_n^o) - \sigma/\epsilon_0)/\epsilon$. The electrostatic solver neglects any space charge effects and assumes that the non-neutral and ambipolar layers of the liquid are thin (see section 3.3).

Summarizing, the model solves for nine variables : the jet radius (h), the liquid surface velocity (u_α), the liquid axis velocity (u_0), the surface charge density (σ), the normal outside electric field (E_n^o), the tangential outside electric field (E_t), the liquid potential (ϕ), the pressure at the axis (P_0) and the pressure at the liquid surface (P_α).

The equations are solved in a sequential fashion, first the time dependent equations (e.g. mass, momentum, and surface charge relaxation) are advanced in time for a given number of iterations while the electric fields are kept constant. The electric fields are updated, (which requires a non-local matrix calculation) and the cycle is repeated until the system is fully converged to steady state.

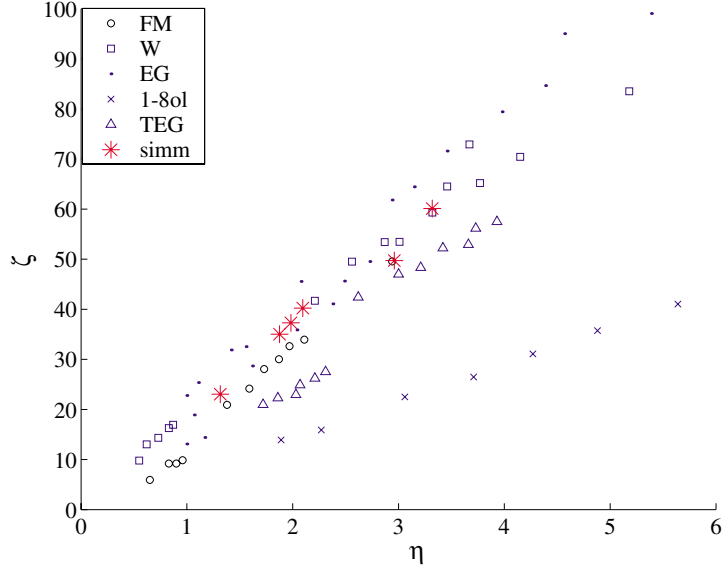


Fig. 2. Dimensionless spray current ζ versus η comparison between experimental and numerical data. Experimental values from de la Mora[1]. Numerical data based on baseline properties for different flow rates.

3 Results and discussion

In the following, we use some of the notation and non-dimensional variables of Fernandez de la Mora[1]. In particular, the flow rate (Q) is reported in terms of the dimensionless variable η and the current is reported in terms of the dimensionless group ζ :

$$\eta = \sqrt{\frac{\rho K Q}{\gamma \epsilon \epsilon_0}}, \quad \zeta = \frac{I}{\gamma (\epsilon_0 / \rho)^{1/2}}. \quad (5)$$

The baseline fluid for our calculations has the properties of Formamide, with density $\rho = 1130 \text{ kg/m}^3$, viscosity $\nu = 3.33 \times 10^{-6} \text{ m}^2/\text{sec}$, surface tension coefficient $\gamma = 0.050 \text{ N/m}$, conductivity $K = 0.001 \text{ Si/m}$, and relative permittivity $\epsilon = 111$. The nozzle radius has been set to $h_0 = 10 \mu\text{m}$ and the collector is at a distance $L = 150 \mu\text{m}$ from the nozzle. The boundary condition for the charge density at the nozzle is set as $\sigma_0 = 0$, and the flow rate (Q) is specified. The applied voltage is set according to an approximate formula for the minimum starting voltage

$$V = \sqrt{\frac{\gamma h_0}{\epsilon_0}} \ln \left(\frac{4L}{h_0} \right) \quad (6)$$

which for the baseline data give 970 Volts.

3.1 Flow rate parameter study

Figure 2 shows the comparison between experimental data of Fernandez de la Mora for multiple solutions and our simulation. It can be seen that the numerically computed currents compare quite well to the experimentally observed values of de la Mora. These results are quite encour-

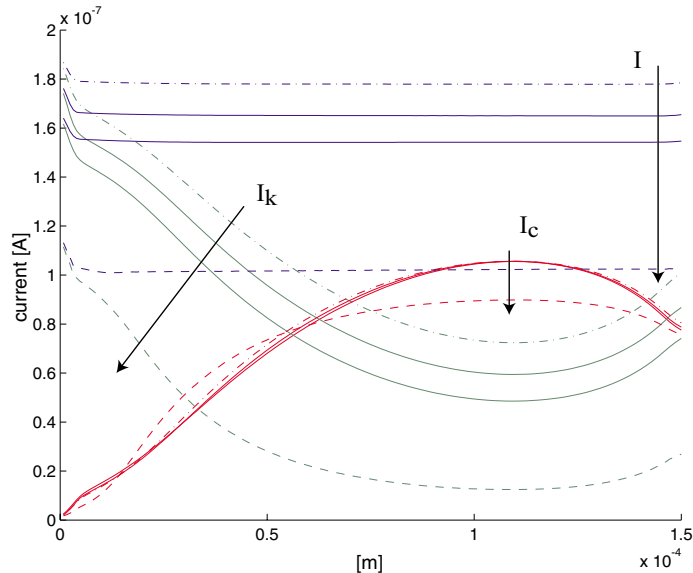


Fig. 3. Convection (I_c), conduction current (I_k) and total current ($I = I_c + I_k$) for Formamide ($K = 1 \times 10^{-3} Si/m$, $\epsilon = 111$) at various flow rates (arrows point to $\eta \rightarrow 1$)

aging, although more checks against experimental values need to be done to further ascertain the validity of our computational results.

Figure 3 shows how the dominant electric current mechanism varies along the cone-jet for various flow rates. It can be seen that as the flow transitions from the cone to the jet the current changes from a conduction dominated behavior to a mixed regime with both conduction and convection of charge. The unexpected result is that, contrary to most existing models, the conduction current does not seem to vanish in the jet, except when minimum flow is approached. To our knowledge, only the results of Yan *et al*[10] have also shown finite conduction currents. It is also interesting to note that the convection current shows only a weak dependence to changes in η (flow rate).

Finally we show the results for the remaining variables of our model. Figure 4 shows the jet radius (h), mean velocity (u) and surface charge density (σ), liquid potential (ϕ), normal outside Electric field (E_n^o) and the tangential electric field (E_t) as they progress from the nozzle to the collector. From these results it is apparent that a qualitative change in the flow behavior occurs as $\eta \rightarrow 1$. The transition region becomes smaller, the flow velocity increases dramatically and the electrostatic behavior changes considerably. It can be seen that for the $\eta = 1.34$ results the potential in the cone region remains almost constant, once the cone becomes a jet the potential changes rapidly until it reaches zero at the collector. The consequences of this behavior affect quite noticeably the electric fields. The maximum values for the electric fields coincide with the point where the convection and conduction currents equal each other. The sudden increase of both electric fields near the collector is due to end boundary condition which sets the liquid potential to zero. Computations using a total length of $300\mu m$ (instead of the $150\mu m$ of the data sets of Figure 4) show that the gradients at the end of the jet simply translate downstream leaving the cone and the transition regions essentially unchanged.

Initial results have been obtained for a modified baseline fluid ($K = 1 \times 10^{-3} Si/m$, $\epsilon = 10$). These results can be seen in Figure 5 and Figure 6. The current results for this second set, contrary to the previous high dielectric constant data set, show a strong variation of the convection current with η (flow rate). In this case the conduction current tends to zero in the jet as analytical models predict. The slope $f(\epsilon) \equiv d\zeta/d\eta$ as defined by Fernandez de la Mora [1] has an experimental value of $f(\epsilon) \simeq 6.3$ to 7.5 which compares well to our results of $f \simeq \zeta/\eta \approx 7$.

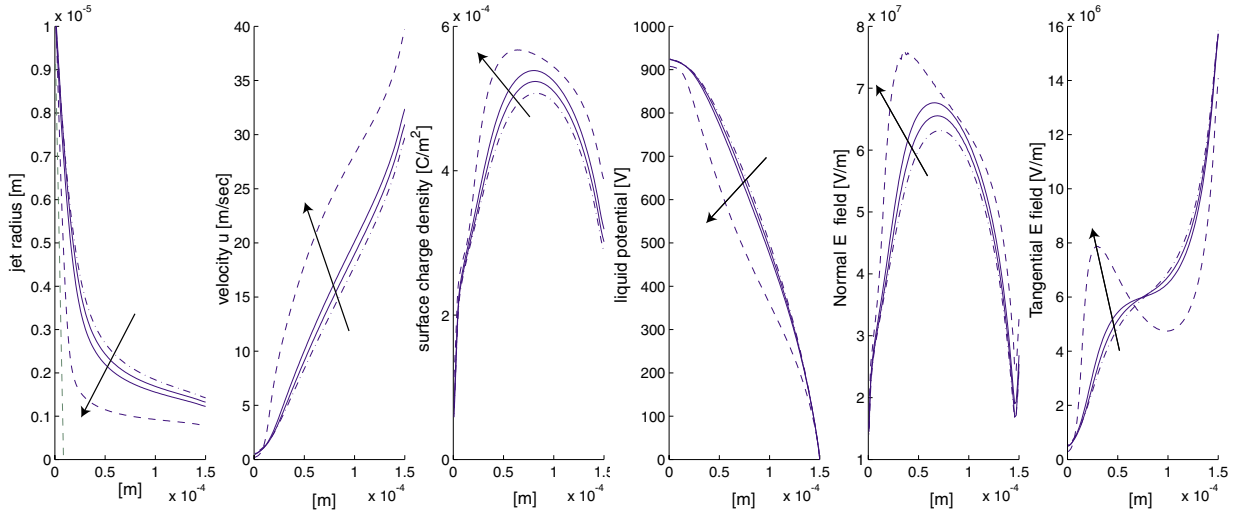


Fig. 4. Data progression for Formamide ($K = 1 \times 10^{-3} Si/m$, $\epsilon = 111$) for various flow rates $\eta = 2$ (dash-dot line) to $\eta = 1.34$ (dashed line). Applied voltage 970 V, collector at $150\mu m$

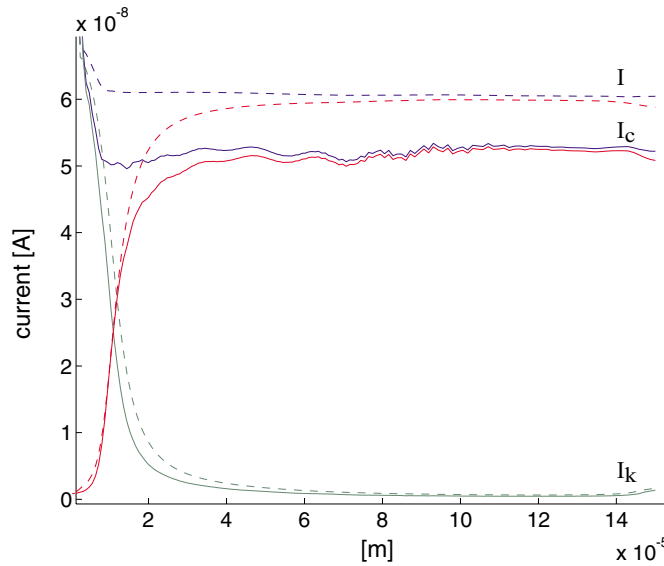


Fig. 5. Convection (I_c), conduction current (I_k) and total current ($I = I_c + I_k$) for modified Formamide ($K = 1 \times 10^{-3} Si/m$, $\epsilon = 10$) at two flow rates ($\eta = 1.69$ solid line) and $\eta = 1.96$

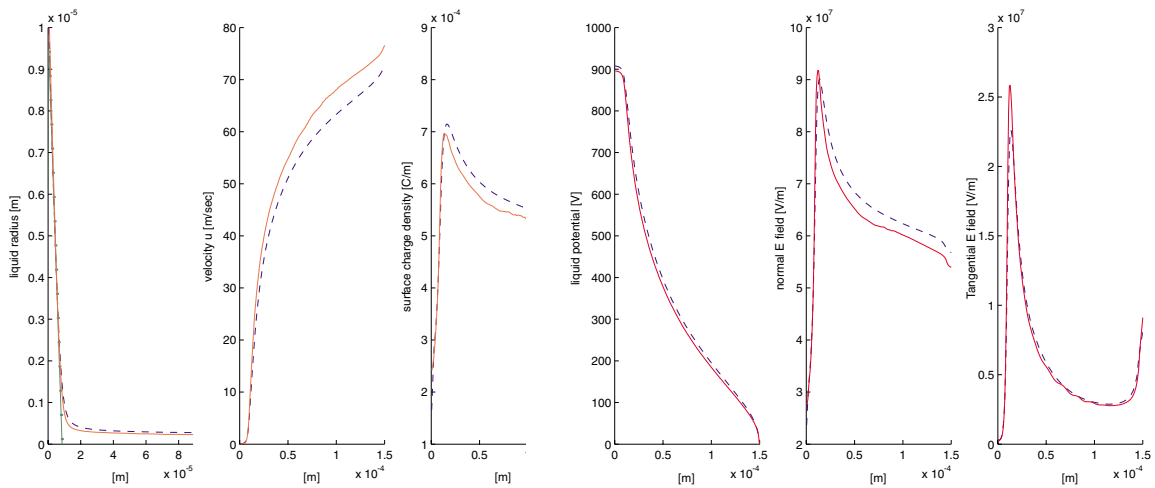


Fig. 6. Results for the modified baseline fluid with $\epsilon = 10$. $\eta = 1.69$ (solid line) and $\eta = 1.96$.

A second point of interest is that the cone region for both η (flow rate) values matches Taylor's angle ($\alpha_T = 49.2^\circ$) whereas the case with $\epsilon = 111$ shows smaller angles ($\alpha < \alpha_T$). It should be pointed out that this data set has not reached steady state yet, but the trends and qualitative behavior of the variables are not expected to change considerably. Further investigation is under way to better understand these results and explore in more detail the effect of the dielectric permittivity (ϵ) on the colloidal jet.

3.2 Energy tracking

In this section we show an energy analysis for the case $\eta = 1.34$ (dashed line in Figure 4) with baseline properties and an operating voltage of 970 V. We calculate the power input of the system by multiplying the extraction voltage by the total resulting current. This power is used for accelerating the flow, setting up the cone-jet shape (surface formation), and some of it is dissipated by viscous stresses, and Joule heating. In our case we present the energy analysis in terms of voltage $V = Power/I$. The sum of all the voltage contributions should ideally be the original extraction voltage, thus conserving energy.

The kinetic voltage is given

$$V_k = \frac{Q\rho}{I}u_{z=L}^2 \quad (7)$$

where I is the total current, Q the flow rate, ρ the density and u is the exit velocity. This voltage is used to accelerate the fluid to its final velocity. For the $\eta = 1.34$ test case it accounts for 66% of the energy usage. The second contribution to the voltage, with 24% is due to Joule heating. This voltage is defined by

$$V_\Omega = \frac{K}{I} \int_0^L \frac{2\pi(hE_t)^2}{1 + \cos(\alpha)} dz. \quad (8)$$

The third contribution is the energy needed to overcome surface tension and set the shape of the liquid jet, which in this case takes 9% of the available power. The formula for this voltage is given by:

$$V_\gamma = \frac{\gamma\pi hu}{I}. \quad (9)$$

The remaining contribution is that due to viscous shear stresses :

$$V_\mu = \frac{\mu}{I} \int_0^L (u')^2 dz. \quad (10)$$

which only accounts for $< 1\%$. Adding up all the different contributions the applied potential should be recovered. In reality a small percentage, in the order of 1- 3% of the applied potential is unaccounted for. This "lost" energy may be due to numerical diffusion, and the fact that the simulation has not settled completely to steady state.

3.3 Ion transport analysis

The component E_n of the outer field normal to the surface of the liquid is reduced by a factor ϵ on crossing the surface, due to the instantaneous polarization of the surface dipoles. The field $E_s = E_n/\epsilon$ at the liquid side of the surface pushes positive ions toward the surface and negative ions away from the surface, leading to a non-neutral layer that, on reaching its equilibrium, would screen the bulk of the liquid from the surface field. The structure and development of this layer, and of a thicker quasineutral layer of ambipolar diffusion that it may induce further into the liquid, are analyzed here on the basis of a non-stationary one-dimensional model. The correspondence between this model and the actual stationary but spatially evolving layers around the surface of the liquid in the bulk-to-surface current transfer region is straightforward when the thickness of the layers is small compared with the radius of the jet. Then it suffices to replace $\partial/\partial t$ by $v_s\partial/\partial s$ in the equations below, where s and v_s are the distance along the surface and the velocity of the liquid at the surface. The correspondence is less simple and only qualitative when the thickness of the layers is of the order of the radius of the jet.

In the one-dimensional model, assuming a fully dissociated 1-1 electrolyte, the densities of positive and negative ions, n^\pm , and the electric field E satisfy

$$\frac{\partial n^\pm}{\partial t} = \frac{\partial}{\partial x} \left(\mp \kappa^\pm n^\pm E + D^\pm \frac{\partial n^\pm}{\partial x} \right) \quad (11a, b)$$

$$\frac{\partial E}{\partial x} = \frac{e}{\epsilon\epsilon_0} (n^+ - n^-) \quad (12)$$

where x is the distance to the surface, negative in the liquid, κ^\pm are the mobilities of the positive and negative ions, and $D^\pm = (kT/e)\kappa^\pm$ are their diffusivities. At the surface, in the absence of ion evaporation and neglecting the variation of the charge of the inner Stern layer,

$$x = 0 : \quad j^\pm = 0, \quad E = E_s = E_n/\epsilon, \quad (13)$$

where $j^\pm = \pm \kappa^\pm n^\pm E - D^\pm \partial n^\pm / \partial x$ are the number fluxes of the ionic species. In the liquid away from the surface

$$x \rightarrow -\infty : \quad n^+ = n^- = n_0, \quad (14)$$

where n_0 is the concentration of the neutral solution. Initial conditions and a law giving the time dependence of the surface field E_s should be specified to complete the formulation of the problem. These, however, will not enter the qualitative discussion that follows.

The well-known stationary solution of (11)–(14) for a constant E_s can be written as

$$\sqrt{\frac{n_0}{n^+}} = \sqrt{\frac{n^-}{n_0}} = \tanh \left[\arg \tanh \sqrt{\frac{n_0}{n_s^+}} - \frac{x}{2^{1/2}\lambda_D} \right], \quad \frac{E}{E_D} = \lambda_D \frac{d \ln(n^+/n_0)}{dx}, \quad (15)$$

where n_s^+ , the density of positive ions at the surface, is given by

$$\frac{n_s^+}{n_0} = 1 + \frac{E_s}{E_D} \sqrt{\frac{1}{2} + \frac{E_s^2}{16 E_D^2} + \frac{E_s^2}{4 E_D^2}}. \quad (16)$$

Here $\lambda_D = (\epsilon\epsilon_0 kT/e^2 n_0)^{1/2}$ is the Debye length and $E_D = kT/e\lambda_D$.

The excess of positive charge and the defect of negative charge in the stationary layer are

$$C^+ = \int_{-\infty}^0 (n^+ - n_0) dx \quad \text{and} \quad C^- = \int_{-\infty}^0 (n_0 - n^-) dx, \quad (17)$$

respectively, whose values scaled with $\lambda_D n_0$ depend only on E_s/E_D . For small values of E_s/E_D , leading to $(n_s^+ - n_0)/n_0 \approx E_s/\sqrt{2}E_D \ll 1$, equations (17) give $C^+ \approx C^-$. In any case, $C^\pm = O(\epsilon\epsilon_0 E_s/e)$.

The time it takes to establish this stationary layer, for example if E_s were switched abruptly from zero, can be estimated from (11) and (12). The balance of all the terms of these equations during a transient reads, in orders of magnitude,

$$\frac{\Delta n}{t_e} = \frac{\kappa n_0 E}{\delta} = D \frac{\Delta n}{\delta^2} \quad \text{and} \quad \frac{E_s}{\delta} = \frac{e \Delta n}{\epsilon\epsilon_0}, \quad (18)$$

where Δn , δ and t_e are the characteristic values of $(n^+ - n^-)$, the thickness of the layer and the duration of the transient, to be determined from these order of magnitude balances, and κ and D are the characteristic values of the mobilities and diffusivities, taken to be of the same order for the two ionic species. The balances (18) yield

$$\frac{\Delta n}{n_0} = \frac{E_s}{E_D}, \quad \delta = \lambda_D, \quad t_e = \frac{\epsilon\epsilon_0}{en_0\kappa}. \quad (19)$$

The first two of these results could have been anticipated from the stationary solution (15)–(16), and the third gives a characteristic time of the order of the electric relaxation time of the liquid evaluated with the conductivity $K = en_0(\kappa^+ + \kappa^-)$ of the neutral solution.

The estimates (19) are valid for $E_s/E_D \ll 1$, but the surface layer develops a two-tiered structure when $E_s/E_D \gg 1$. Then negative ions are depleted from a thin sublayer where $E = O(E_s)$ and $n = O(n_f)$, with $n_f = n_0 (E_s/E_D)^2 \gg n_0$. The characteristic thickness of this sublayer is kT/eE_s , which is the Debye length evaluated with n_f instead of n_0 . This is followed by a layer of thickness λ_D where E/E_D and $\Delta n/n_0$ are both of order unity. The thin sublayer is responsible for most of the excess of positive charge, which is $C^+ = O(\epsilon\epsilon_0 E_s/e)$, while $C^- = O(\epsilon\epsilon_0 E_D/e)$.

In the experiments with NaI in Formamide ($\epsilon = 111$) that motivated the numerical computations of this paper, $n_0 \approx 9.3 \times 10^{22} \text{ m}^{-3}$ was required to attain a conductivity $K = 10^{-3} \text{ S/m}$. In these conditions $\lambda_D = 4.14 \times 10^{-8} \text{ m}$ and $E_D = 10^6 \text{ V/m}$. The non-neutral layer is therefore thin compared with the radius of the jet observed numerically ($\approx 10^{-6} \text{ m}$) and experimentally, and E_D is slightly larger than the highest surface field E_n/ϵ , which is about $8 \times 10^5 \text{ V/m}$ at the conditions of minimum flow rate.

The relaxation time t_e is to be compared with the characteristic time of variation of the surface field, which is the residence time of the liquid in the bulk-to-surface current transfer region, t_r say, when the model is applied to this region. If $t_e/t_r \ll 1$, then the layer around the surface screens the bulk of the liquid from the surface field. If t_e/t_r is not small, then the quasi-static layer has no time to develop and fields of order E_n/ϵ should be expected in the liquid.

The surface layer is not strictly stationary when $t_e/t_r \ll 1$; rather it undergoes a quasisteady evolution in which C^\pm in (17) vary in a time of order t_r . The required inflow and outflow of charge to the surface layer originate in a thicker quasineutral region of ambipolar diffusion. There (12) reduces to the quasineutral approximation

$$n^+ = n^- = n \quad (20)$$

and the sum and difference of the two equations (11) divided by D^\pm give

$$\frac{\partial n}{\partial t} = \bar{D} \frac{\partial^2 n}{\partial x^2} \quad \text{and} \quad \frac{\partial n}{\partial t} = \bar{\kappa} \frac{\partial}{\partial x} (nE), \quad (21)$$

where

$$\bar{D} = \frac{2}{1/D^+ + 1/D^-} \quad \text{and} \quad \bar{\kappa} = \frac{2}{1/\kappa^- - 1/\kappa^+}. \quad (22)$$

Boundary conditions for equations (21) are $n = n_0$ for $x \rightarrow -\infty$ and the conditions of matching with the thinner non-neutral layer

$$\frac{dC^\pm}{dt} = \pm j^\pm = \kappa^\pm n E \mp D^\pm \frac{\partial n}{\partial x}, \quad (23)$$

to be imposed effectively at $x = 0$. Defining $\alpha = (dC^+/dt) / (dC^-/dt)$, which can be replaced by unity when $E_s/E_D \ll 1$, these conditions can be rewritten as

$$\frac{D^+ + D^-}{D^+ - \alpha D^-} \bar{D} \frac{\partial n}{\partial x} = \frac{\kappa^+ - \kappa^-}{\kappa^+ + \alpha \kappa^-} \bar{\kappa} n E = \frac{dC^-}{dx}. \quad (24)$$

The characteristic thickness of the region of ambipolar diffusion is $\delta_a = (\bar{D} t_r)^{1/2}$, from the first equation (21). Here t_r is the time available for the diffusion layer to grow, which is the residence time of the flow in the current transfer region in the application at hand. As can be seen, $\lambda_D/\delta_a = O(t_e/t_r)^{1/2} \ll 1$. The characteristic variation of n across the layer of ambipolar diffusion can be estimated as $\Delta n_a = O[(\delta_a/\bar{D}) (dC^-/dt)]$, from the equality of the first and last terms of (24). Using here $dC^-/dt = O(\Delta n \lambda_D/t_r)$, with Δn given by (19), and the estimate of δ_a above, this result becomes $\Delta n_a/n_0 = O[(\Delta n/n_0)(t_e/t_r)^{1/2}] \ll 1$. The characteristic value of the electric field is $E/E_D = [(E_s/E_D)(t_e/t_r)] \ll E_s/E_D$, from (21) and the estimates above.

Strictly, the value of n_0 to be used in (15)–(17) for the non-neutral layer does not coincide with the concentration in the bulk of the liquid, because of the intervening ambipolar diffusion layer. The difference, however, is small in view of the small value of $\Delta n_a/n_0$. For the same reason, the conductivity of the liquid can be approximated by the constant conductivity at $n = n_0$ everywhere outside the non-neutral layer.

The estimate of δ_a needs to be changed when it comes out larger than the radius of the jet. Then ambipolar diffusion extends to the whole cross-section of the jet, of characteristic radius r_s say, and the variation of the charge density required to feed the non-neutral surface layer is $\Delta n_a/n_0 = O[(\Delta n/n_0)(\lambda_D/r_s)]$.

4 Conclusions and future work

Numerical results for a Formamide solution with conductivity $K = 10^{-3}$ Si/m and flow rates $1.34 \leq \eta \leq 2.1$ have been presented. The numerical results conserve mass, charge and energy and the predicted current compares quite well with published experimental data of de la Mora [1]. Further examination of our results shows that (except near the minimum flow) there still exists a finite conduction current in the jet downstream of the transition region. It is also shown that the convection current behaves as a weak function of the flow rate for the baseline liquid

properties. It was found that the minimum stable flow occurs when the asymptotic downstream conduction current approaches zero, and, at least for the parameters of this study, that this limit is reached at $\eta \approx 1$. Finally for the case of $\eta = 1.34$ we have shown a power usage breakdown which accounts for 97% of the available power. On the other hand, for a liquid with ϵ reduced to 10, the conduction current is seen to vanish shortly after the transition (for $1 \leq \eta \leq 2$ at least), and the convection current now does vary with $Q^{1/2}$.

The analytical section of the paper addressed, the behavior of the non-neutral layer and ambipolar layer of a liquid subjected to a normal electric field at the surface. Order of magnitude arguments and calculations (for our baseline properties) conclude that the non-neutral layer is thin (a few percent) compared to the jet diameter. This conclusion justifies the use of a constant conductivity K to model charge transport in the liquid.

Acknowledgements: This work was supported under AFOSR Grant F49620-01-0398. Mitat Birkan monitor

References

- [1] Fernandez de la Mora J. ,and Loscertales, I. G., *The current emitted by highly conducting Taylor cones*, Journal of Fluid Mechanics, Vol. 260, pp. 155-184, 1994.
- [2] Hohmann, M. , Shin M., Rutledge G.,and Brenner M., *Electrospinning and electrically forced jets. II. Applications*,Physics of Fluids, Vol. 13 #8, pp. 2221-2236, 2001.
- [3] Martinez-Sanchez, M., Fernandez de la Mora, hruby, V., Gamero-Castano, M., Khayms, V.,*Research on colloid thrusters*,IEPC99-014, 26th International Electric Propulsion Conference, Oct. 17-21, 1999. Kitakyushu, Japan
- [4] Hartmann, R. P. A., Brunner, D. J., Camelot, D. M. A., Marijnissen,J. C. M. , and Scarlett, B., *Electrohydrodynamic atomization in the cone-jet mode physical modeling of the liquid cone and jet*,Journal of Aerosol Science, V. 30, No. 7, pp 823-49, 1999.
- [5] Eggers, J. ,and Dupont, T. F., *Drop formation in a one-dimensional approximation of the Navier-Stokes equations*, Journal of fluid mechanics,V. 262 pp 205-221, 1994.
- [6] Carretero, J. A., Martinez-Sanchez M. , *Quasi-one-dimensional numerical simulation of a single-emitter colloidal jet.*,38th Joint Propulsion Conference and Exhibit. 7-10 July 2002 Indianapolis Indiana AIAA-2002-3812
- [7] Landau, L. D., Lifshitz, E. M. , *Electrodynamics of continuous media*, Pergamon Press L.T.D., second impression, 1966
- [8] Lozano, P., and Martinez-Sanchez, M., *Jets and Sprays emitted from colloid thrusters- experiments and modeling*, Proc. 3rd International Conference on Spacecraft Propulsion, Cannes, 10-13 October 2000.
- [9] Hohmann, M., Shin, M., Rutledge, G.,and Brenner M., *Electrospinning and electrically forced jets. II. Applications*,Physics of Fluids, Vol. 13 #8, pp. 2221-2236, 2001.
- [10] Yan, F., Farouk, B., and Ko, F., *Numerical modeling of an electrostatically driven liquid meniscus in the cone-jet mode*,Journal of Aerosol Science, Vol. 34, pp. 99-116, 2003.